Submitted to the International Europhysics Conference on High Energy Physics HEP99,
Tampere, Finland, July 1999

# Test of the Standard Model in high $\mathrm{P_T}$ jet production at HERA

H1 Collaboration

**Abstract**

Following the observation by H1 of unexpected events with jets, high $P_T$ leptons and large missing transverse momentum, we explore final states with similar kinematic configurations but only high $P_T$ jets in the final state. The data sample comprises all available $e^+p$ data collected in 1994 to 1997. The cross sections for two and three jet production as function of jet transverse momentum and multi-jet invariant mass are compared with QCD predictions for multi-jet events. No significant deviations from expectation are found.

**Abstract: 157u**
**Parallel sessions: 1, 6**
**Plenary sessions: 1, 6**

**Electronic Access: http://www-h1.desy.de/publications/**

# 1 Introduction

In [1] we have reported the observation of events containing an isolated charged lepton with large transverse momentum $P_T$ together with large missing transverse momentum $P_{T,\text{miss}}$ in $e^+p$ scattering data collected in 1994–1997 at the HERA collider. While some of the events are naturally explained by Standard Model processes such as $W^\pm$ production, three of these events also have a hadronic system with large transverse momentum and show atypical kinematic properties compared to expectation. In all three events the charged lepton is a muon, and no scattered electron is detected.

In view of these events with a charged lepton and $P_{T,\text{miss}}$, we here investigate corresponding final states with two jets or more of similar kinematic configuration and no scattered electron in the central part of the detector. The resulting cross sections as functions of jet transverse momentum and two or three jet invariant mass are compared to a leading order (LO) QCD prediction for the photoproduction of jets.

# 2 Event Selection and Reconstruction

The data sample used was collected in 1994-1997 in $e^+p$ scattering at a centre-of-mass energy of $300\,\text{GeV}$ at the HERA collider. The H1 detector is explained in detail in [2]. The main detector components used in this analysis are the Liquid Argon Calorimeter (LAr), the backward[1] SPACAL calorimeter, the Central Jet Chamber and the luminosity system. The integrated luminosity where these detector components were fully operational corresponds to $35.7 \pm 0.5 pb^{-1}$.

The triggers used for this selection are based on energy depositions in the LAr calorimeter and on the tracking system. The trigger efficiency, which is monitored by using events with SPACAL triggers as a reference sample, exceeds $95\%$ everywhere. The error on the trigger efficiency is $4\%$ at most.

The hadronic energy of events is reconstructed by using a combination of energy depositions in the calorimeters and tracks in the central jet chamber. The energy calibration for jets was deduced from test beam data and, in situ, from kinematic constraints in a large sample of deep inelastic neutral current events with jets of similar transverse momentum. Jet energies are corrected to their true values. The remaining systematic uncertainty on the energy scale is $\pm 4\%$ including a $2\%$ contribution which is correlated from bin-to-bin.

The phase space for the cross section measurements is restricted by the following cuts:

$$Q^2 < 4\,\text{GeV}^2 \qquad \text{and} \qquad y < 0.9 \tag{1}$$

The cut on $Q^2$ corresponds to the inner acceptance of the SPACAL calorimeter. Events with an electron identified in the LAr calorimeter are rejected. To further reduce the contamination from neutral current deep inelastic interactions, events are also removed if an energy of more than $5\,\text{GeV}$ is measured in the electromagnetic part of the SPACAL calorimeter, if the energy

[1]The backward ($-z$) direction denotes the direction of the positron beam momentum, which corresponds to a polar angle of $\theta = 180^0$.

of a jet containing tracks is contained to more than $90\%$ in the electromagnetic part of the LAr calorimeter or if a track in the jet points to a crack in the electromagnetic section of the LAr calorimeter. The cut on $y$, which also removes deep inelastic scattering events, corresponds in the event selection to $y_{JB} = \sum_h (E - P_z)_h / (2E_e^0) < 0.9$, where the sum runs over all hadrons in the event and $E_e^0$ denotes the positron beam energy of $27.6\,\mathrm{GeV}$. In addition a set of cuts is applied against cosmic muons and the missing transverse momentum $P_{T,\mathrm{miss}}$ is restricted to $P_{T,\mathrm{miss}} < 20\,\mathrm{GeV}$.

Jets are defined by applying the inclusive $k_T$ algorithm [3] for massless jets to all hadrons in the detector frame. Jets are accepted in the angular range

$$-0.5 < \eta_{jet} < 2.5 \tag{2}$$

where $\eta_{jet} = -\ln \tan \theta_{jet}/2$ is the pseudorapidity of the jet axis. Jets are sorted with respect to transverse momentum such that

$$P_T^{jet1} > P_T^{jet2} > P_T^{jet3} > \ldots \tag{3}$$

The following jet event samples are defined:

- The 2-jet sample includes events with at least two jets found with transverse momenta of

$$P_T^{jet1} > 25\,\mathrm{GeV} \qquad \text{and} \qquad P_T^{jet2} > 15\,\mathrm{GeV}. \tag{4}$$

- For the 3-jet sample, the same cuts are applied as for the 2-jet sample. In addition a third jet must exist with

$$P_T^{jet3} > 10\,\mathrm{GeV}. \tag{5}$$

After these selections 5146 events are found in the 2-jet sample, and 946 events in the 3-jet sample.

# 3 Cross Section Measurement

The hadron level cross sections in the region of phase space defined by eq. 1 to 4 and, for the 3-jet sample by eq. 5, are obtained from the measured event rates by correcting for acceptance losses and inefficiencies using events generated by the monte carlo programs PYTHIA 5.7 [4] and HERWIG 5.9 [5].

Both programs are based on leading order QCD matrix elements for the description of hard parton scattering processes, and include initial- and final-state parton showers and initial state photon radiation from the electron in leading logarithmic approximation. The programs differ however largely in their mechanism of parton showering, in the fragmentation model applied and in their concepts of simulating additional interactions between partons of the proton remnant and of the photon remnant in resolved processes.

For the proton and photon the GRV–LO parton density parametrisations [7] are used which are known to be compatible with jet rates in photoproduction events at much lower $P_T^{jet}$[8].

Large samples of events generated with PYTHIA and HERWIG were subject to a detailed simulation of the H1 detector, and then reconstructed and analysed as the data.

Both the PYTHIA and the HERWIG simulation reproduce well the energy flow measured in the data close to and in between jets, and are in fair agreement with the data concerning the angular and transverse momentum distributions of jets. Both programs are thus applied in the unfolding procedure to the hadron level cross section. Pythia has been used for the central results, whereas the difference (typically $10\%$) between HERWIG and PYTHIA is adopted as a systematic error of the correction procedure.

The background from Neutral Current and Charged Current deep inelastic scattering processes are estimated from monte carlo simulations. The background is found to be always less than $3\%$ and is subtracted on a statistical basis.

The total systematic error is dominated by the uncertainty of the energy calibration in the LAR calorimeter (typically $15-20\%$). This error is added in quadrature to the uncertainty due to the energy calibration in the SPACAL calorimeter, the integrated luminosity ($\pm 1.5\%$), the uncertainty on the trigger efficiency, the size of the background from deep inelastic scattering events and the model uncertainty in the unfolding procedure. Neither bin centre corrections nor radiative corrections are applied.

# 4 Results

Cross sections for the 2-jet sample as functions of $P_T^{jet1}$ of the leading jet and of the average $P_T$ of the two leading jets are shown in Fig. 1 and 2. In the range $\sim 20 < P_T^{jet} <\sim 90\,\mathrm{GeV}$ the cross section falls by three orders of magnitude. Both in shape and normalisation, the data are well described by the GRV–LO parton density, LO QCD matrix elements and parton showers as implemented in PYTHIA 5.7 (see above). This also holds for the invariant mass distribution of the two leading jets in the 2-jet sample as shown in Fig. 3. The QCD prediction for photoproduction of jets is therefore shown to be valid up to the highest transverse momenta observed up to now.

For the 3–jet sample, cross sections as function of the transverse momentum of the third jet $P_T^{jet3}$ and of invariant masses of various jet–jet combinations are shown in Fig. 4 and 5, respectively. Also here normalisation and shape are well described by the leading order expectation with a slight, however insignificant, deviation at the highest masses.

The kinematic configuration of the three atypical muon events would correspond in the 3-jet sample to the case where all three jets have large transverse momenta and are well separated from each other such that invariant masses of jet pairs are large. While no significant deviation is seen in Fig. 4 and 5 it is noted that the QCD prediction yields a considerable number of events also at large $P_T^{jet}$ and invariant jet-jet mass in the inclusive distributions presented here. New mechanisms for jet production therefore have to be identified in more exclusive analysis which will benefit greatly from the understanding of QCD high Pt jet production presented here.

# 5 Conclusion

We have investigated jet production in events without a scattered positron in the central detector in $35.7 pb^{-1}$ of $e^+p$ data collected in 1994–1997. The measured cross sections for two or more jets and three or more jets are compatible within errors with a LO QCD prediction for photoproduction processes. The three jet sample is particularly interesting in view of events observed by H1 with missing $P_T$, high $P_T$ leptons and jets. In view of the considerable number of jet events expected from QCD processes also at large transverse momenta, no firm conclusions can be drawn at the present time on a possible confirmation of this observation in the three jet channel.


# Acknowledgements

We are grateful to the HERA machine group whose outstanding efforts have made and continue to make this experiment possible. We thank the engineers and technicians for their work constructing and maintaining the H1 detector, our funding agencies for financial support, the DESY technical staff for continual assistance and the DESY directorate for the hospitality which they extend to non-DESY members of the collaboration.


# References


[1] H1 Collaboration, C. Adloff *et al*, *Eur. Phys. J.* **C5** (1998) 4, 575-584.

[2] H1 Collaboration, I. Abt *et al*, *Nucl. Instrum. Methods* **A386** (1997) 310 and 348.

[3] S.D. Ellis and D.E. Soper, *Phys. Rev.* **D48** (1993) 3160;
S. Catani, Yu.L. Dokshitzer, M.H. Seymour and B.R. Webber, *Nucl. Phys.* **B406** (1993) 187.

[4] T. Sjöstrand, *Comp. Phys. Commun.***82** (1994) 74;
T. Sjöstrand, CERN-TH-7112-93 (Dec. 1993, revised Aug. 1994).

[5] G. Marchesini *et al*, *Comp. Phys. Commun.*86 (1995) 147.

[6] G. Marchesini and B. Webber, *Nucl. Phys.* **B238** (1984) 1;
G. Marchesini and B. Webber, *Nucl. Phys.* **B310** (1988) 461.

[7] M. Glück, E. Reya, A. Vogt, *Phys. Rev.* **D46** (1992) 1973.

[8] H1 Collaboration, C. Adloff *et al*, *Eur. Phys. J.* **C1** (1998) 97-107.

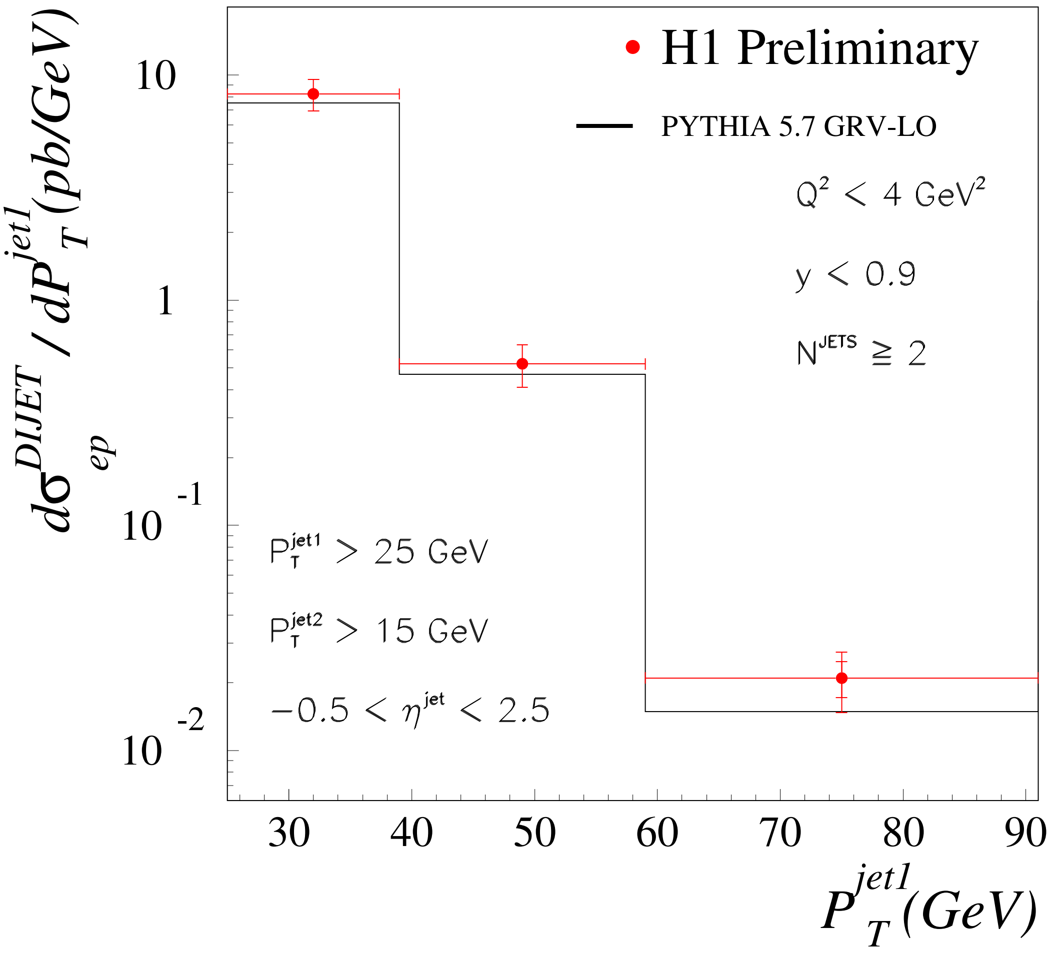


Figure 1: Hadronic cross section for 2-jet production as function of the transverse momentum of the leading jet $P_T^{jet1}$. The inner error bars denote the statistical, the outer error bars the quadratic sum of all statistical and systematic errors of the data. The histogram shows a prediction based on the GRV–LO parametrisation of parton densities and LO QCD matrix elements as implemented in the PYTHIA 5.7 monte carlo.

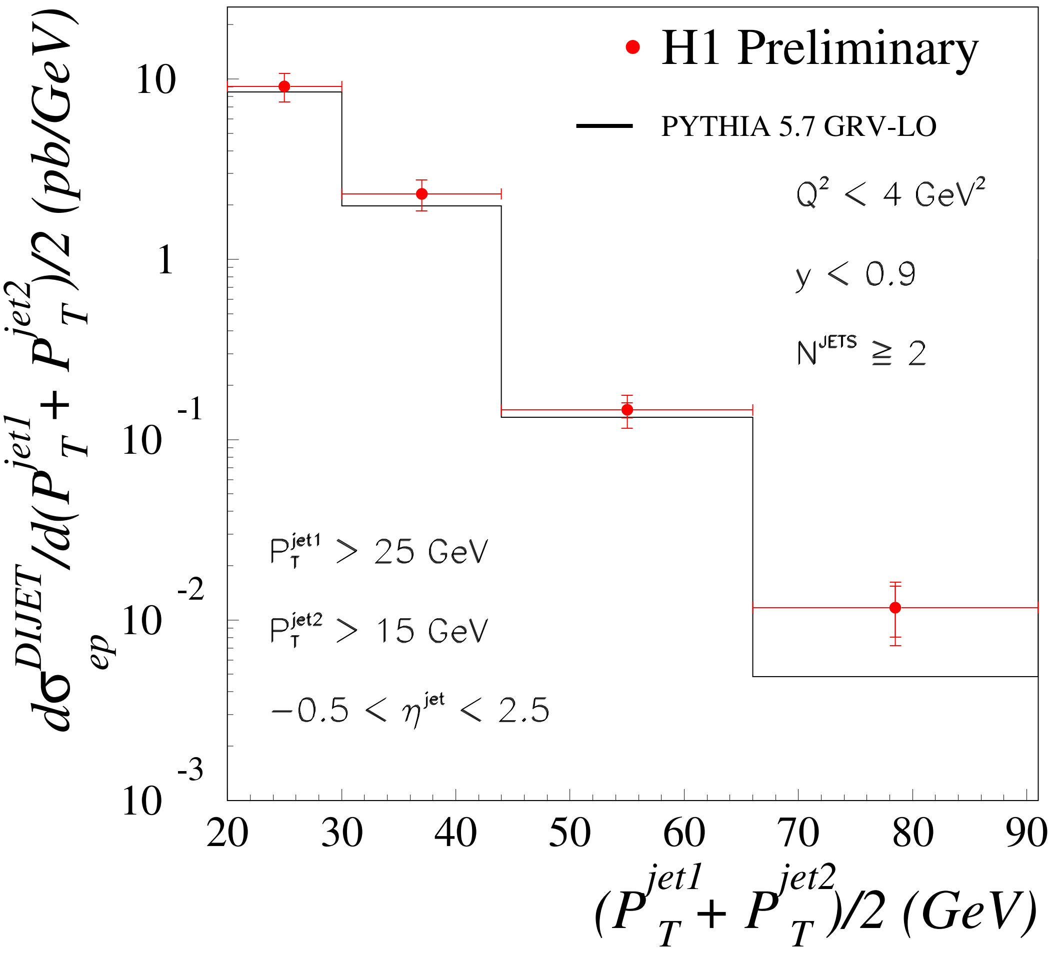


Figure 2: Hadronic cross section for 2–jet production as function of the average transverse momentum of the two leading jets $P_T^{jet1}$ and $P_T^{jet2}$. The inner error bars denote the statistical, the outer error bars the quadratic sum of all statistical and systematic errors of the data. The histogram shows a prediction based on the GRV–LO parametrisation of parton densities and LO QCD matrix elements as implemented in the PYTHIA 5.7 monte carlo.

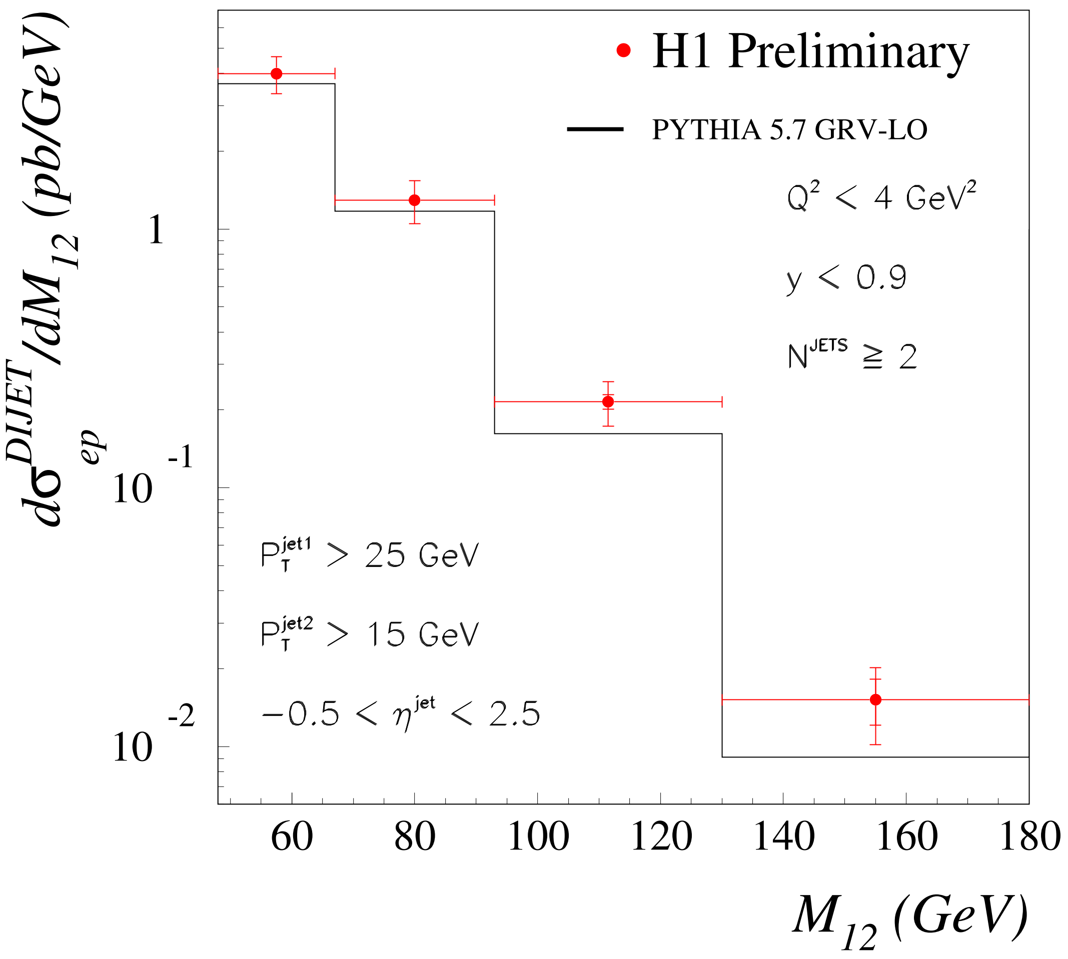


Figure 3: Hadronic cross section for 2–jet production as function of the invariant mass of the two leading jets $M_{12}$. The inner error bars denote the statistical, the outer error bars the quadratic sum of all statistical and systematic errors of the data. The histogram shows a prediction based on the GRV–LO parametrisation of parton densities and LO QCD matrix elements as implemented in the PYTHIA 5.7 monte carlo.

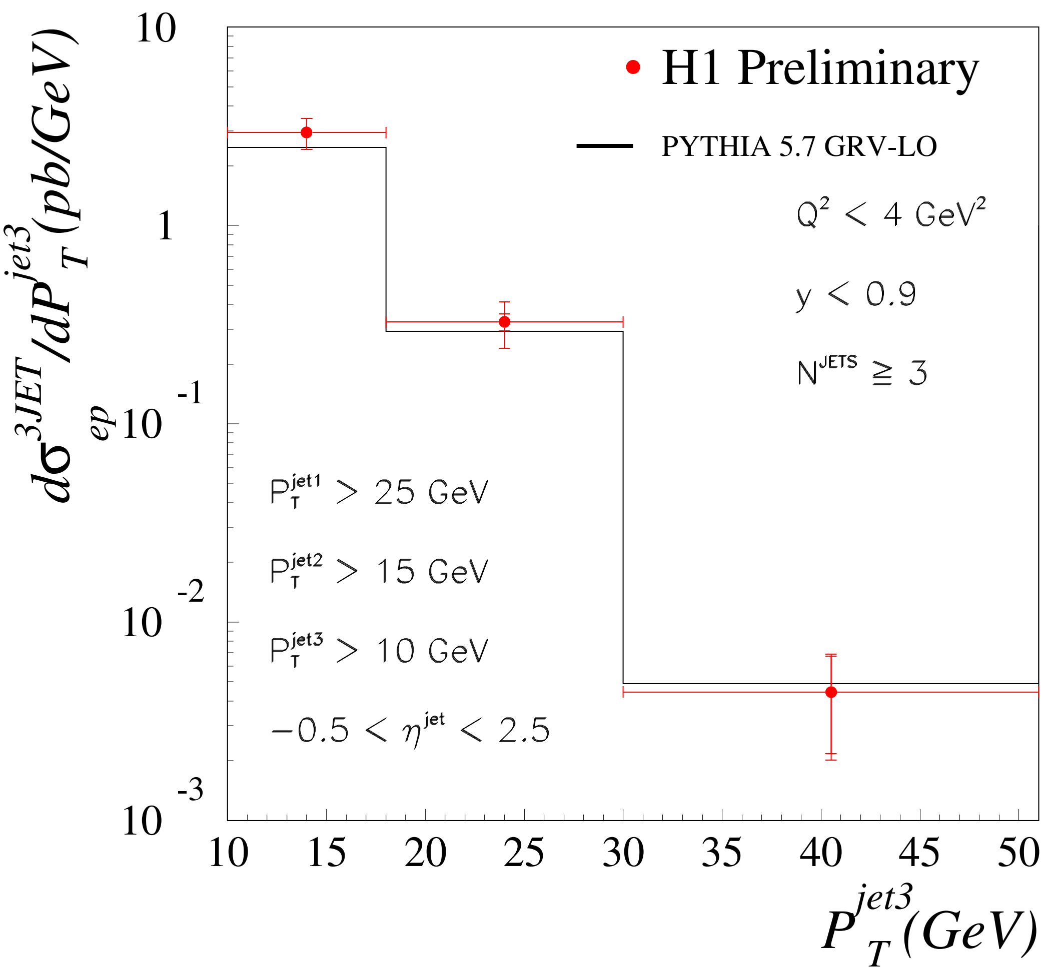


Figure 4: Hadronic cross section for 3–jet production as function of the transverse momentum of the third jet $P_T^{jet3}$. The inner error bars denote the statistical, the outer error bars the quadratic sum of all statistical and systematic errors of the data. The histogram shows a prediction based on the GRV–LO parametrisation of parton densities and LO QCD matrix elements as implemented in the PYTHIA 5.7 monte carlo.

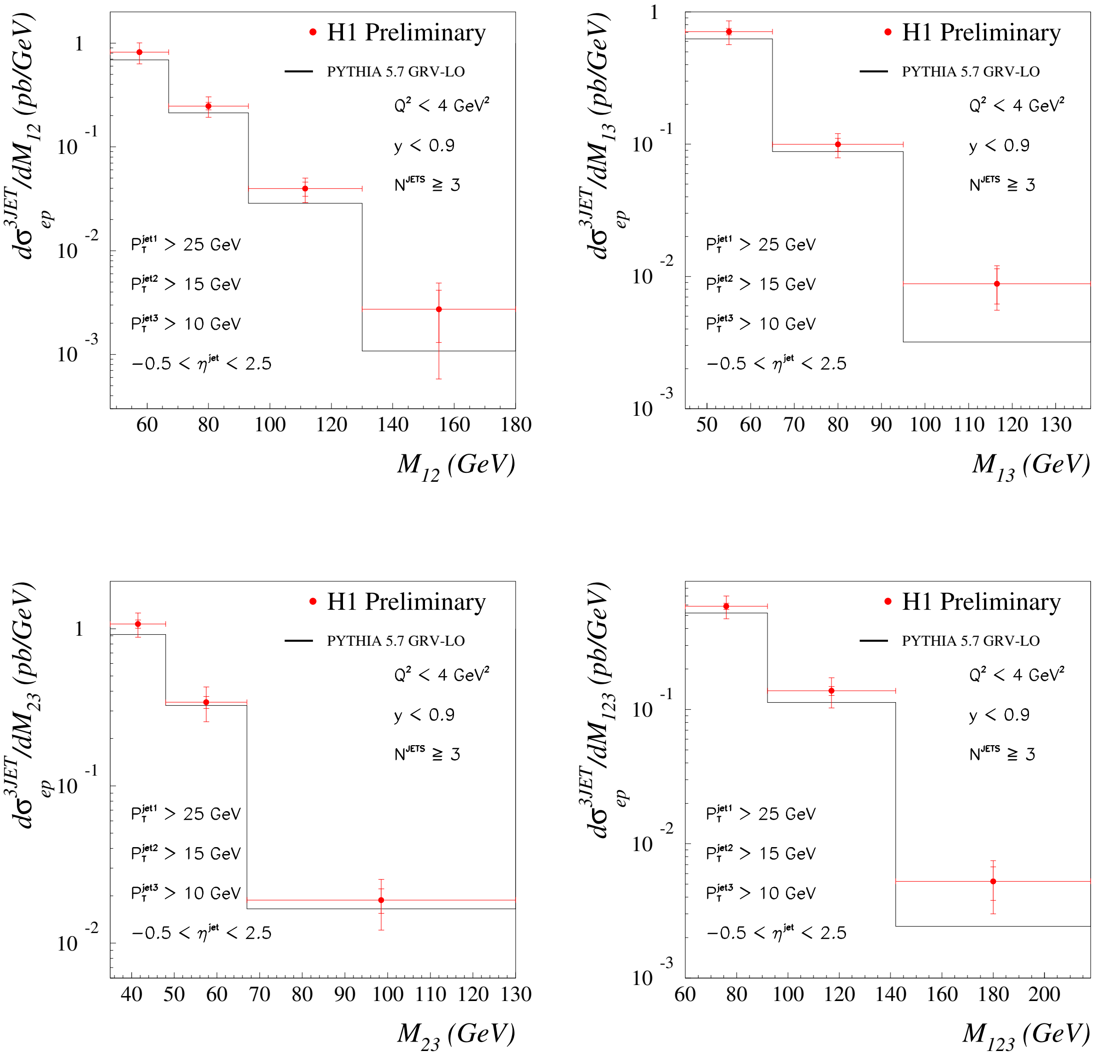


Figure 5: Hadronic cross sections for 3–jet production as function of the invariant mass of the two leading jets $M_{12}$ (upper left), the first and third jet $M_{13}$ (upper right), the second and third jet $M_{23}$ (lower left) as well as all three jets $M_{123}$ (lower right). The inner error bars denote the statistical, the outer error bars the quadratic sum of all statistical and systematic errors of the data. The histogram shows a prediction based on the GRV–LO parametrisation of parton densities and LO QCD matrix elements as implemented in the PYTHIA 5.7 monte carlo.